Supporting Information

"Breast Cancer Cells Transition from Mesenchymal to Amoeboid Migration in Tunable 3D Silk-Collagen Hydrogels"

Amanda S. Khoo, Thomas M. Valentin, Susan E. Leggett, Dhananjay Bhaskar, Elisa M. Bye, Shoham Benmelech, Blanche C. Ip, and Ian Y. Wong.

Rheological Strain Sweeps

Strain sweeps for 0.5 and 2 mg/mL collagen as well as 5 and 10 mg/mL silk hydrogels were performed. These concentrations cover the maximum and minimum concentrations of the composite hydrogels. The linear viscoelastic regime (LVR) extends beyond 1% strain, the strain at which all frequency sweeps were performed in **Figure 2**.

For collagen hydrogels, the yield strain (γ_y) for 0.5 mg/mL ≈4% strain, at which point a slight increase in storage modulus was seen. For 2 mg/mL hydrogels γ_y ≈5% strain at which point a dramatic decrease in storage modulus was seen, indicative of permanent deformation of the hydrogel structure (**Figure S1A**). For silk hydrogels, γ_y ≈1.25% strain for 5 mg/mL hydrogels, at which point a slight decrease in storage modulus was seen. For 10 mg/mL hydrogels, no γ_y was seen over the strain sweep (**Figure S1B**).

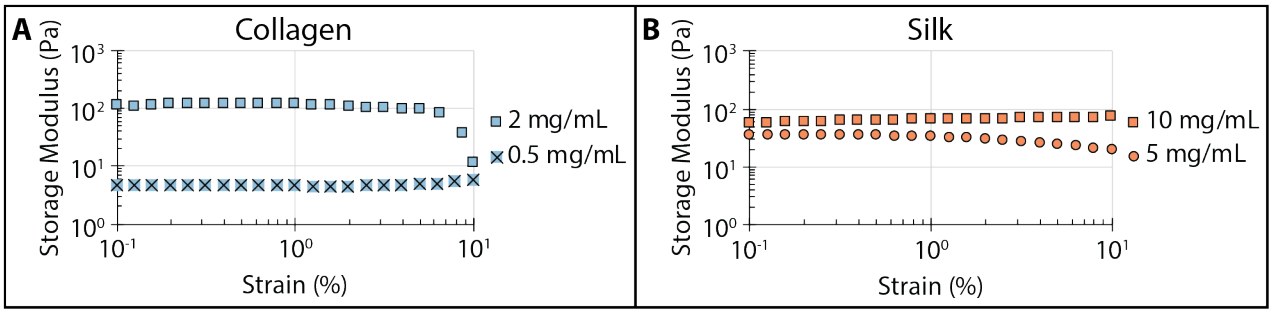

Figure S1: **(A)** Strain sweeps for 0.5 and 2 mg/mL collagen hydrogels. Frequency sweeps in fgr:Fig2 were performed at 1% strain. LVR extends beyond 1% strain. **(B)** Strain sweeps for 5 and 10 mg/mL silk hydrogels. Frequency sweeps in fgr:Fig2 were performed at 1% strain. LVR extends beyond 1% strain.

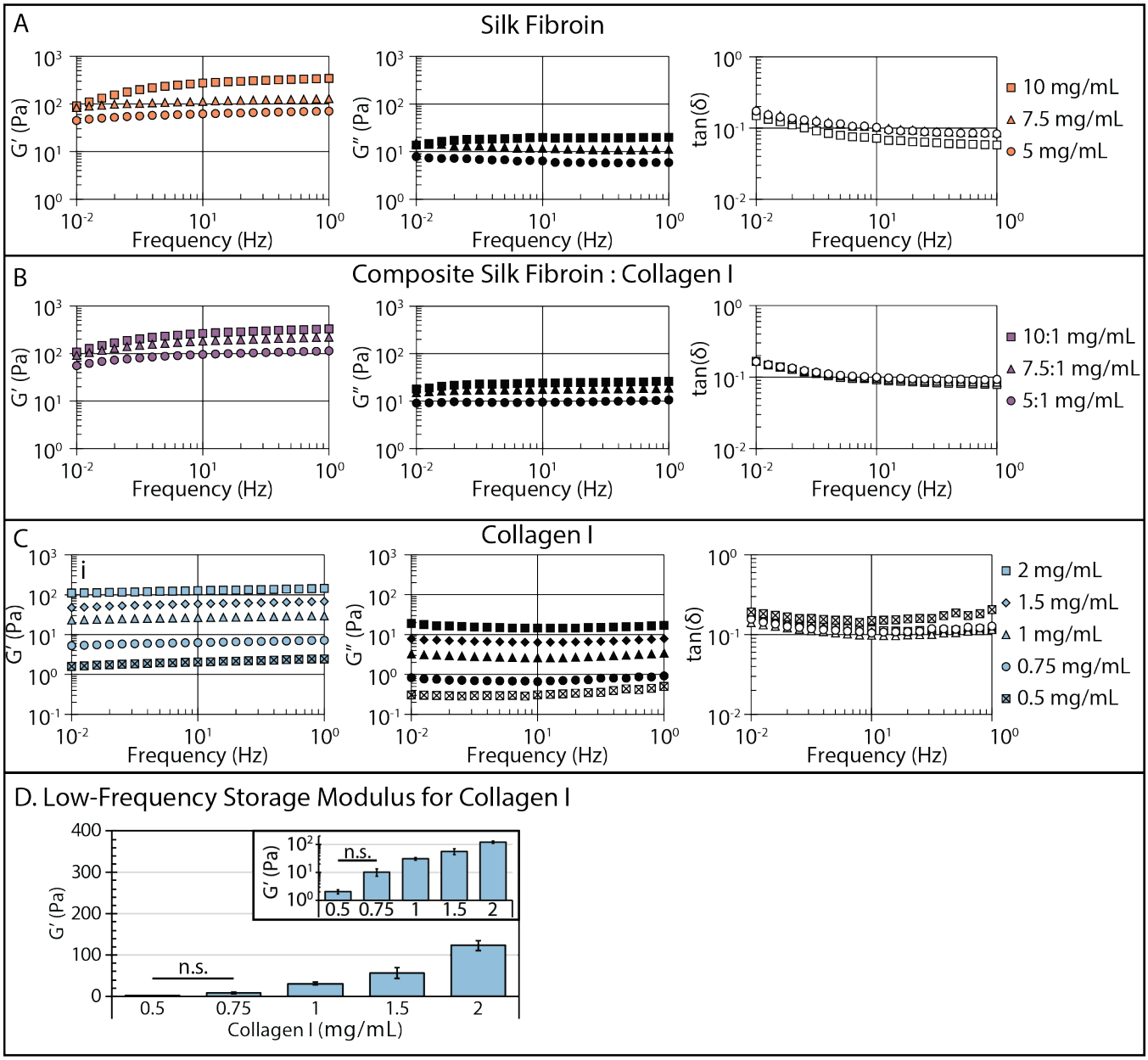

Figure S2: Rheological frequency sweeps and plots of storage modulus (G'), loss modulus (G"), and tan(δ) for **(A)** collagen, **(B)** silk, **(C)** silk : collagen hydrogels, **(D)** and Average storage modulus (n=3) for collagen hydrogels taken at a frequency of 0.1 Hz. Error bars = standard deviation. $p < 0.05$ between means for all conditions unless otherwise indicated (Student's t-test).

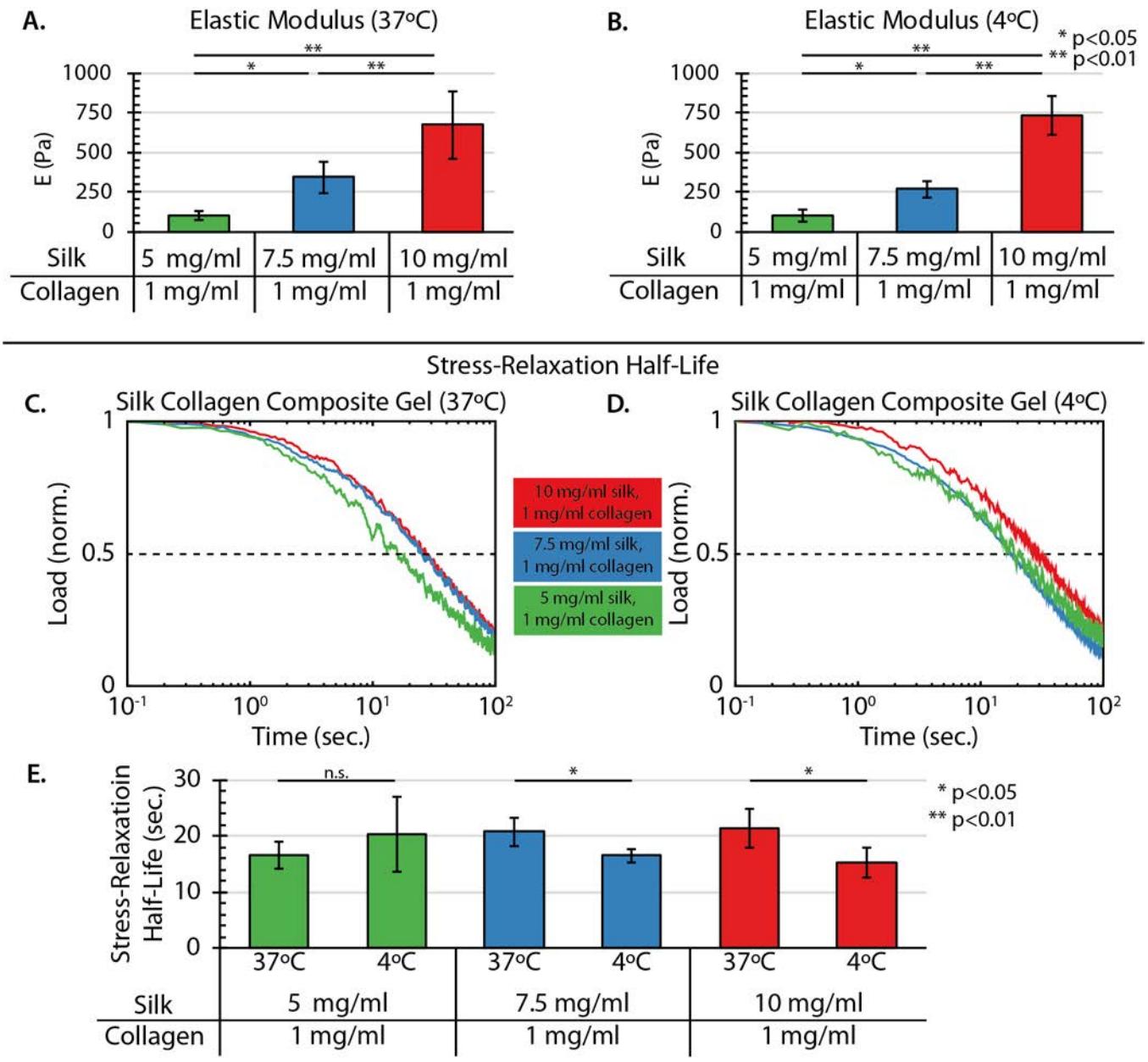

Figure S3: **(A)** Mean elastic modulus for silk : collagen hydrogels incubated at 37°C. Error bars = standard deviation. * $p<0.05$, ** $p<0.01$ (Wilcoxon Krusal-Wallis test with non-parametric multiple comparisons). **(B)** Mean elastic modulus for silk : collagen hydrogels incubated at 4°C. Error bars = standard deviation. * $p<0.05$, ** $p<0.01$ (pair-wise Student's t-test). **(C)** Stress-relaxation plot of silk : collagen hydrogels incubated at 37°C. Load is max-min normalized. * $p<0.05$, ** $p<0.01$ (Wilcoxon Krusal-Wallis test with non-parametric multiple comparisons). **(D)** Stress-relaxation plot of silk : collagen hydrogels incubated at 4°C. Load is max-min normalized. **(E)** Stress-relaxation half-lives for silk : collagen hydrogels incubated at 37°C and 4°C. Error bars = standard deviation.

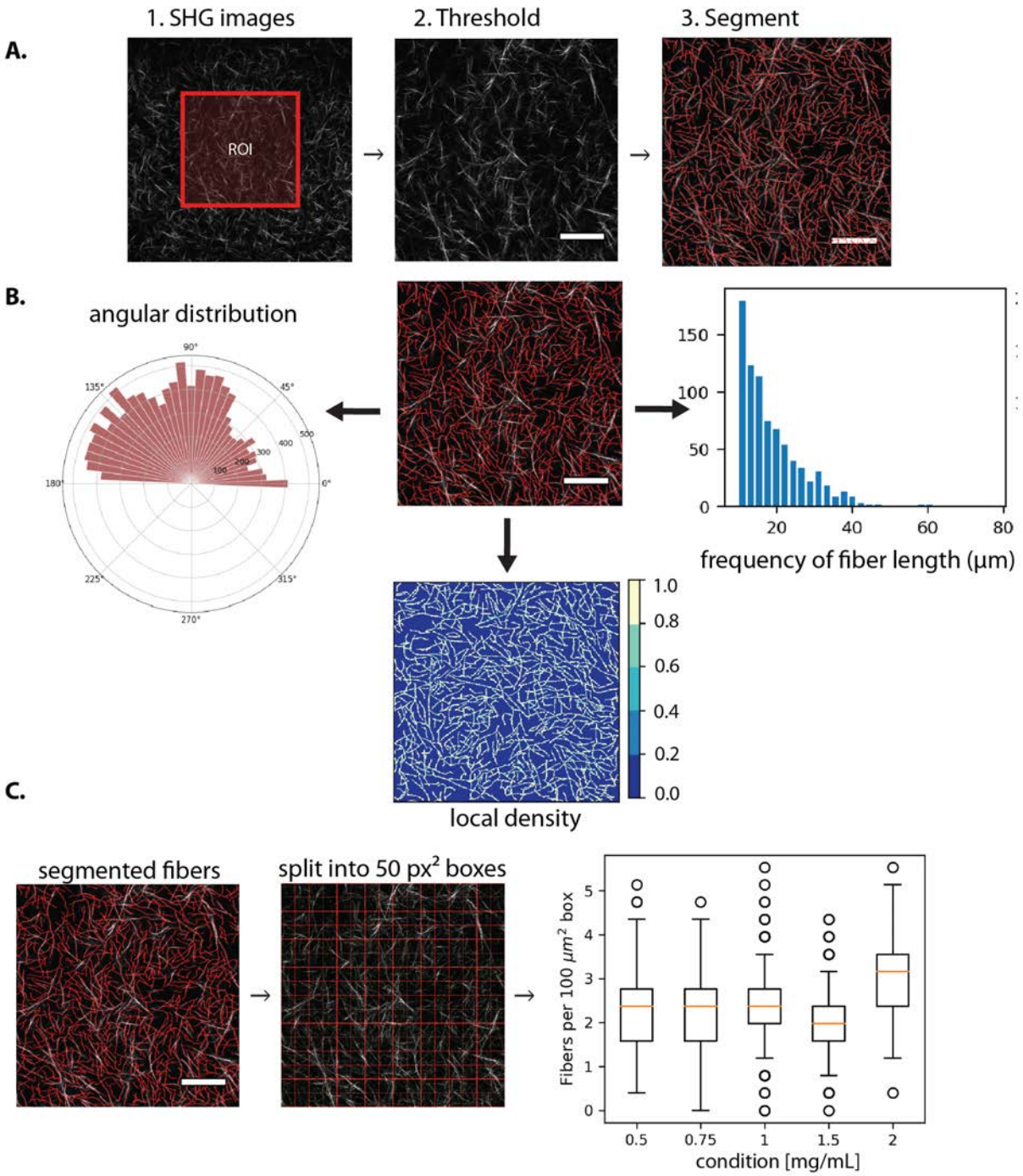

Figure S4: CT-FIRE and CurveAlign workflow and outputs. **A1.** Tif files produced from second harmonic generation are cropped to a center region of interest (red box). **A2.** Image is thresholded to qualitatively view as many fibers as possible, then saved as a jpg and used as ground truth for CT-FIRE parameter optimization. **A3.** Segmented fibers are output as a mask and overlaid on jpg ground truth image. **B.** CT-FIRE outputs can be directly fed into CurveAlign. Subset of useful CurveAlign outputs, including angular distribution of fibers, fiber length, and local fiber density. **C.** Segmented fiber mask was split into 256 50 by 50 pixel boxes and number of unique fibers in each box was counted. Number of fibers in a 100 μm box for collagen only gels. Boxplot shows the 25th, 50th (median) and 75th percentiles. Whiskers span from box to 1.5 x distance between the 25th and 75th quantiles (interquartile range, or IQR). Values outside 1.5 x IQR are plotted as outlier points.

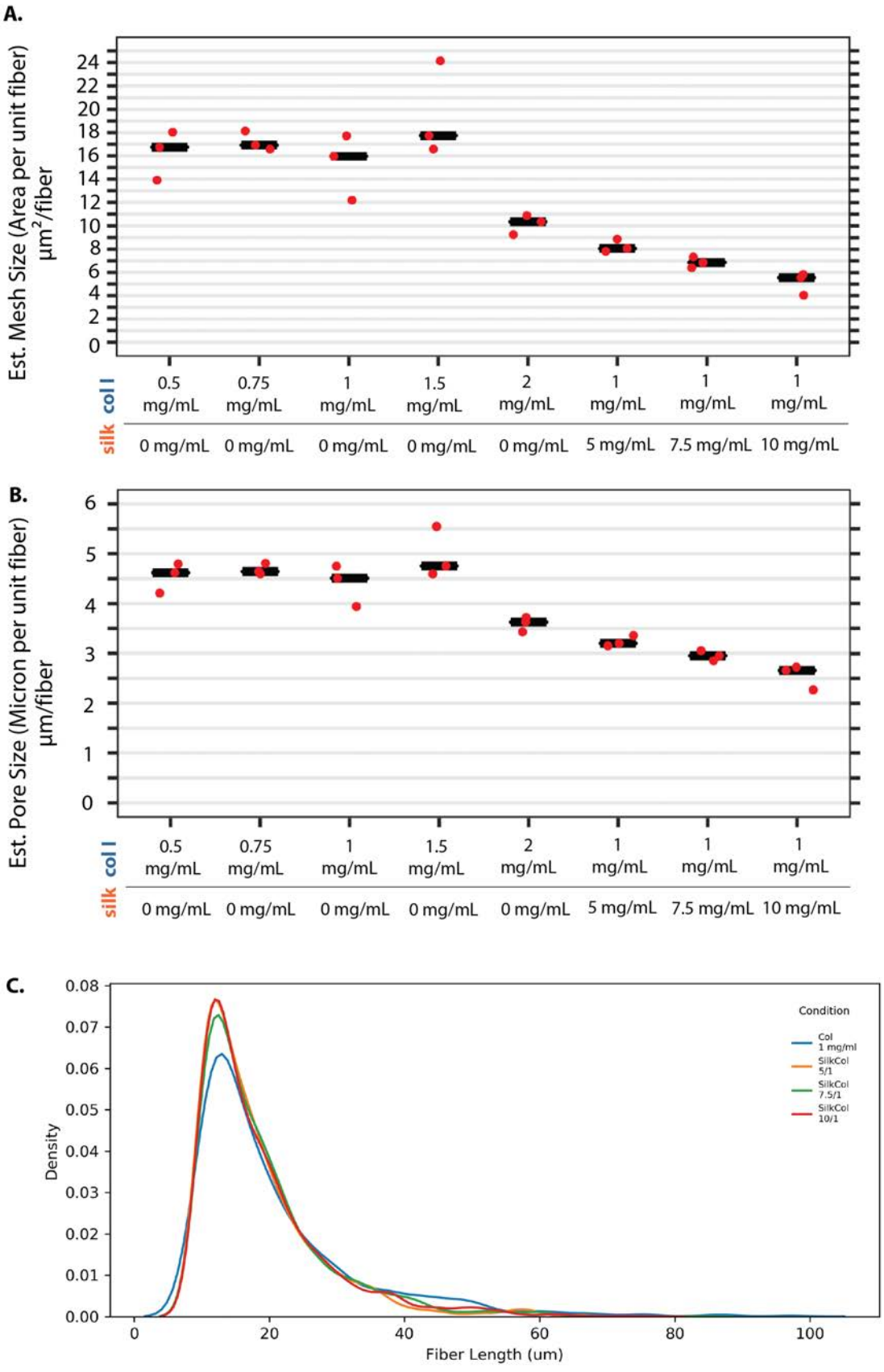

Figure S5: **A.** Mesh area estimate calculated by taking the area of a circle that fits within the average square box that, on average for that image, houses one fiber. **B.** Pore diameter calculated as the square root of the mesh area (in agreement with previous reports).[27] Boxplots show the 25th, 50th (median) and 75th percentiles. Whiskers span from box to 1.5 x distance between the 25th and 75th quantiles (interquartile range, or IQR). Values outside 1.5 x IQR are plotted as outlier points. **C.** Normalized counts of fiber (fragment) lengths. Total collagen concentration is conserved between the 1 mg/mL collagen I only hydrogel (blue) and composite hydrogels with 1 mg/mL (orange, green, red).

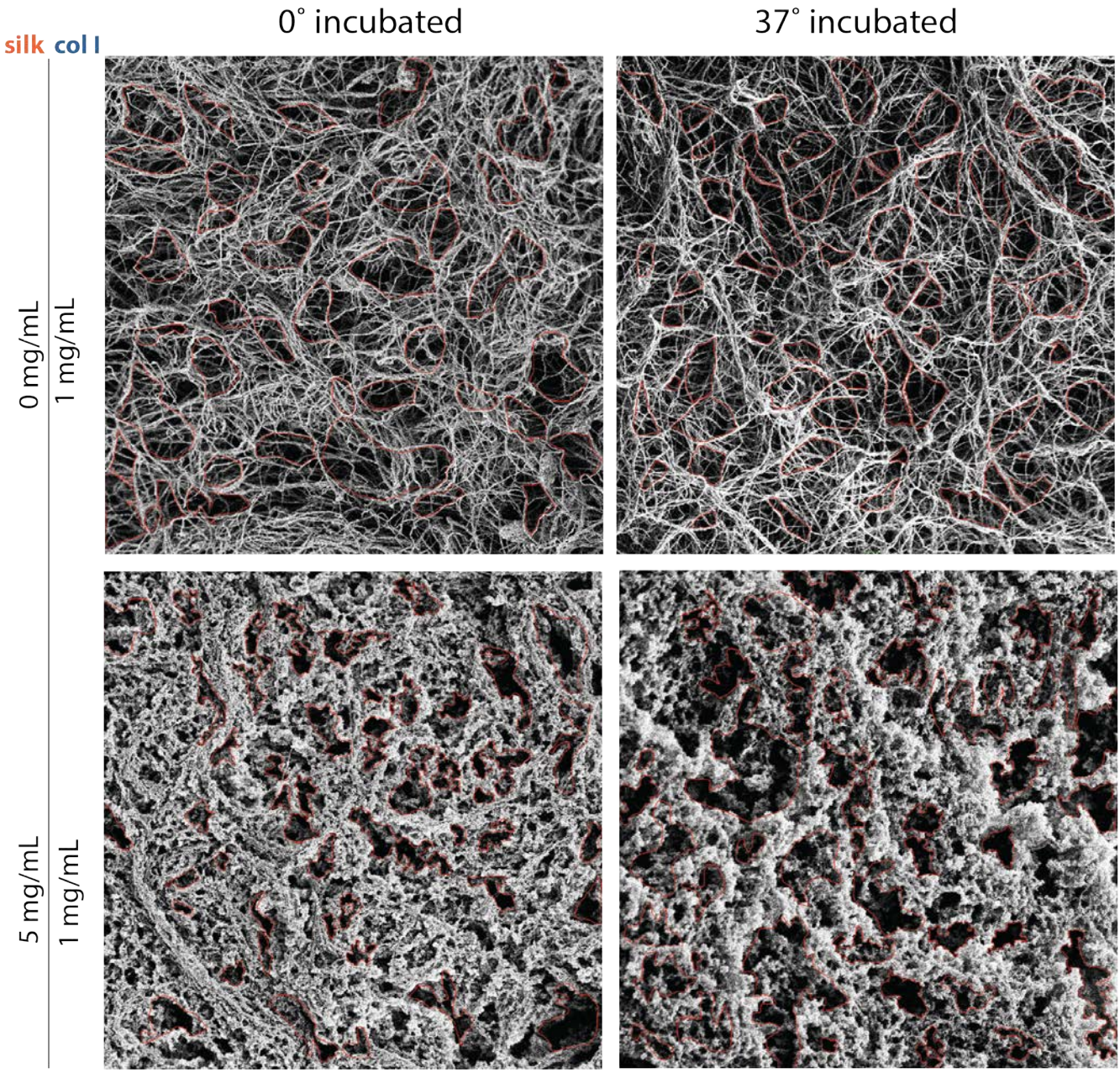

Figure S6: Scanning Electron Microscopy images of 1 mg/ml collagen gels and composite silk-collagen gels. Pore annotations in red overlaid on grey SEM jpegs.

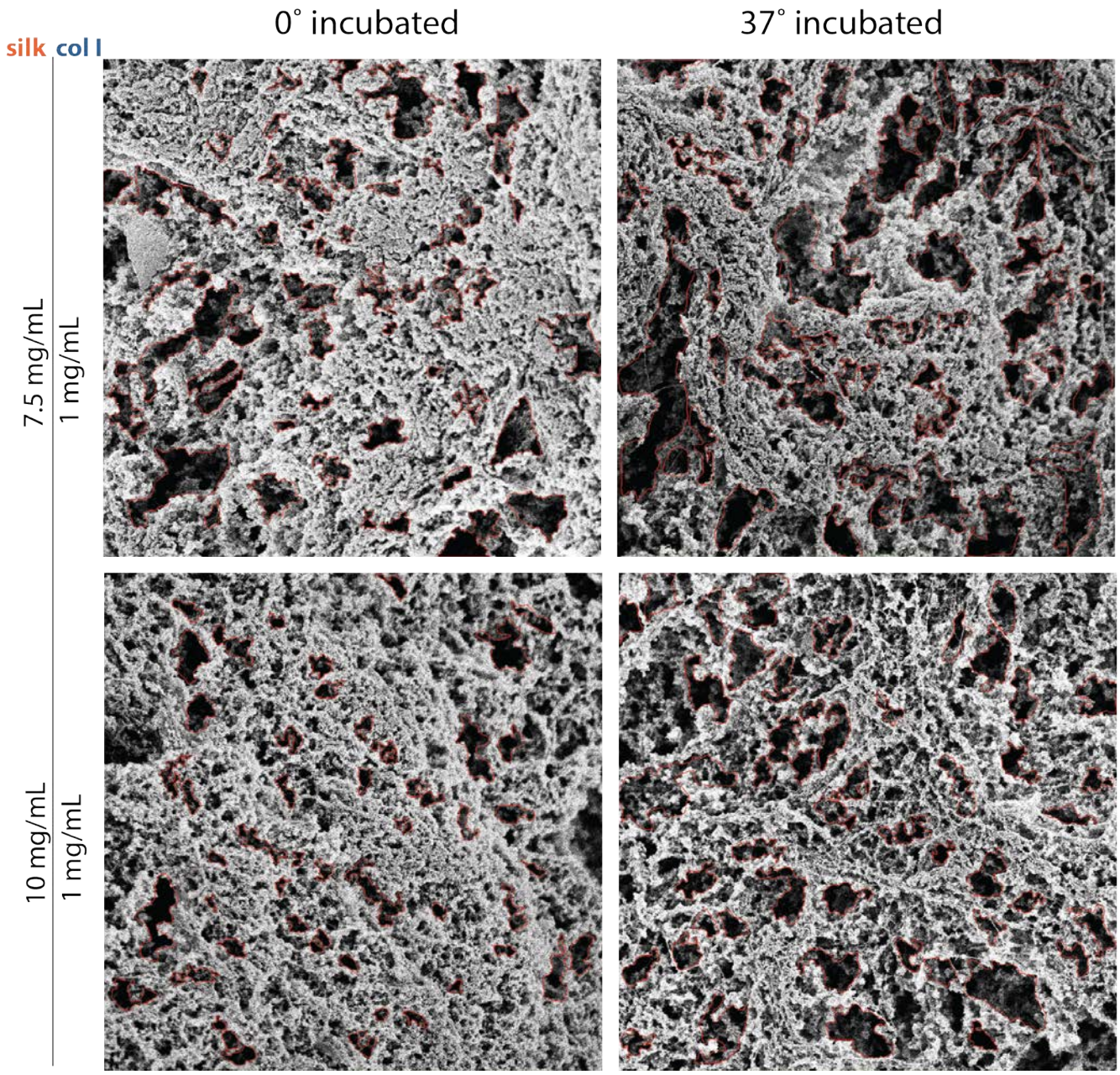

Figure S7: Scanning Electron Microscopy images of composite silk-collagen gels. Pore annotations in red overlaid on grey SEM jpegs.

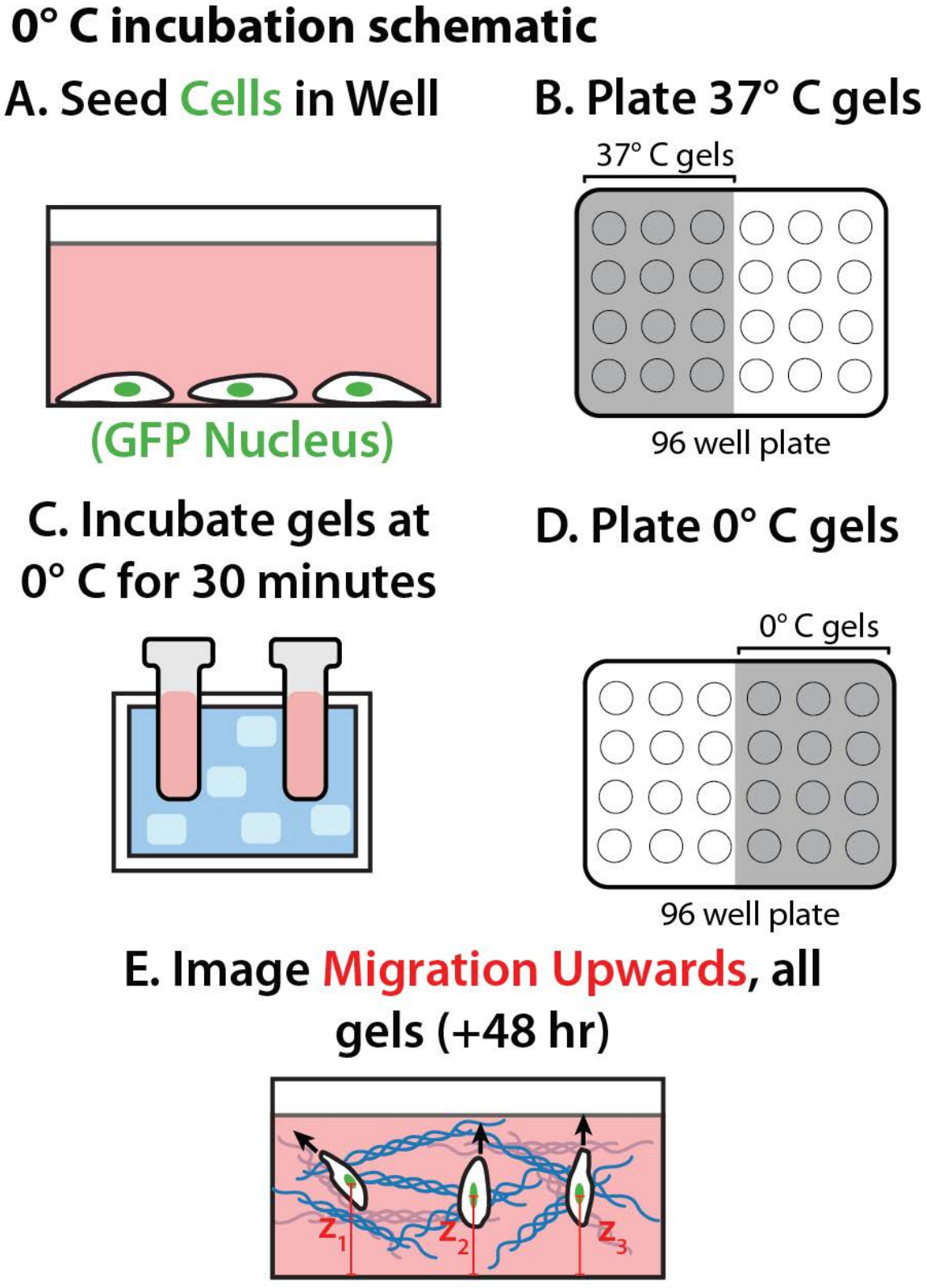

Figure S8: Pre-incubation schematic. (A.) Cells are seeded in a 96 well plate and allowed to adhere. (B.) Precursor gel solutions are created and half of each homogenous gel solution is pipetted into the wells. (C.) The other half of each gel condition is incubated on wet ice for 30 minutes. (D.) Pre-incubated gels are plated onto the well plate. (E.) Polymerized gels topped with media and imaged for 48 hours.

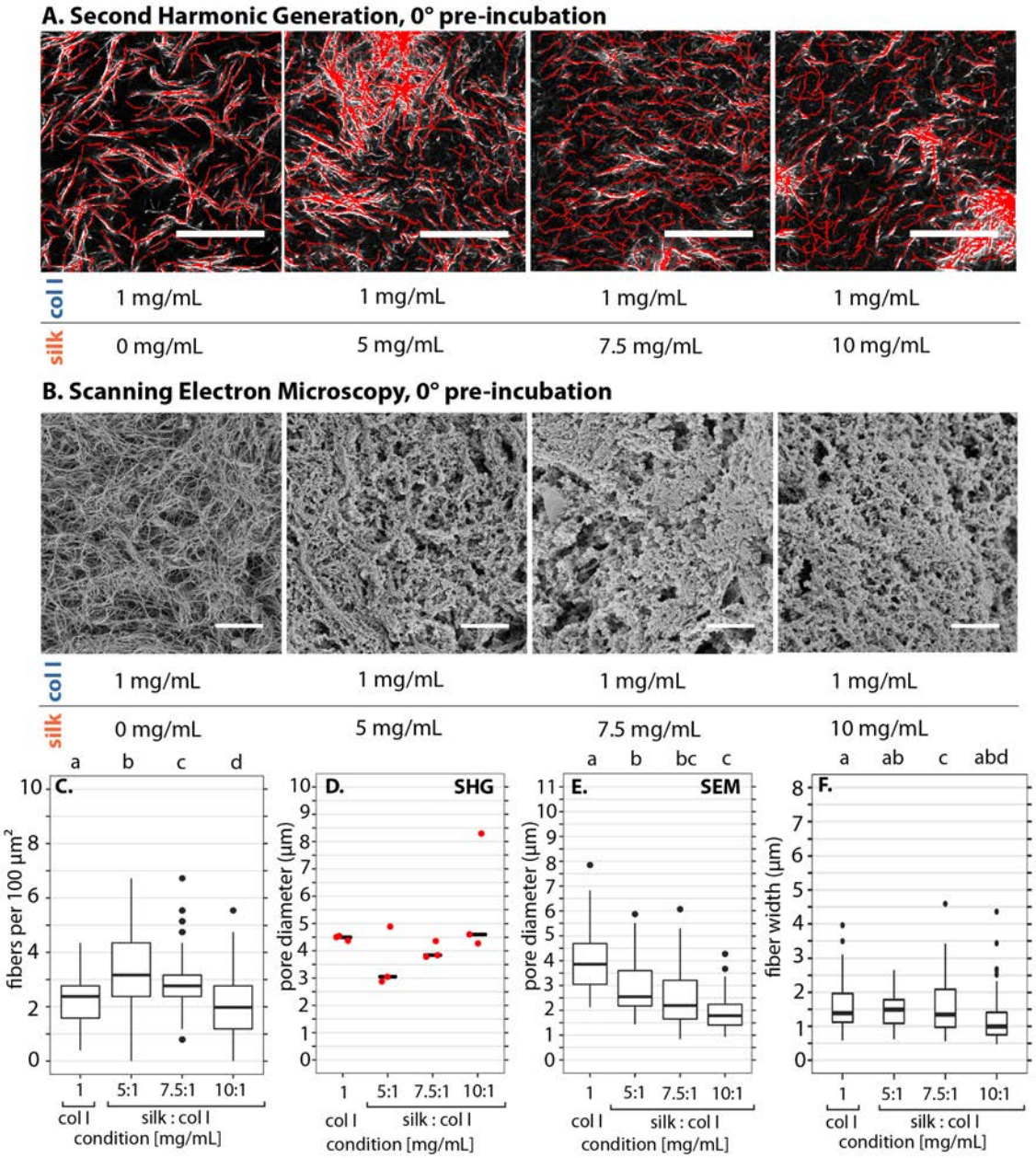

Figure S9: Representative images and analysis for hydrogels incubated at 0 degrees for 30 minutes. (A) Representative second harmonic generation (SHG) microscopy images of collagen I fibrillar architecture for 1 mg/mL collagen I with 0 - 10 mg/mL silk (white), with overlaid fiber detection (red). Scale bar: 50 μm (B) Scanning Electron Microscopy images of 1 mg/ml collagen gels and composite silk-collagen gels. (C) Number of detected collagen I fibers from second harmonic analysis using CurveAlign per 100 Âţm2. Letters denote statistically different groups with $p < 0.05$, using Kolmogorov-Smirnov test corrected for multiple comparisons. (D) SHG pore diameter estimated interpolated for the average box that fits one fiber from CurveAlign density output. Pore diameter here is an estimate for collagen mesh alone in collagen and composite silk collagen gels. (E) SEM pore diameter from 50 pore segmentations from a 50 x 50 micron representative image. Statistic: Multiple comparison t-test corrected for multiple comparisons. (F) Analysis of SHG images for fiber width. Statistical test: Wilcoxen corrected for multiple comparisons. All boxplots show the median with lower (25%) and upper quartiles (75%). Whiskers further extend by 1.5X interquartile range from the lower and upper quartiles, with data points beyond this range plotted as outliers.

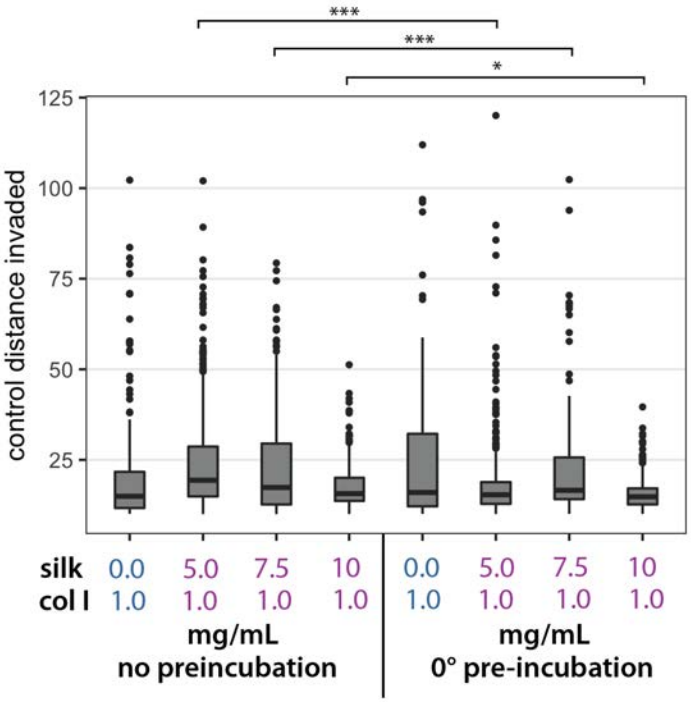

Figure S10: Distance invaded into composite matrices with and without pre-incubation at 0 degrees. Incubation significantly decreases invasion in all composite matrices. Boxplots show the median with lower (25%) and upper quartiles (75%). Whiskers further extend by 1.5X interquartile range from the lower and upper quartiles, with data points beyond this range plotted as outliers. Statistical test: Wilcoxen.

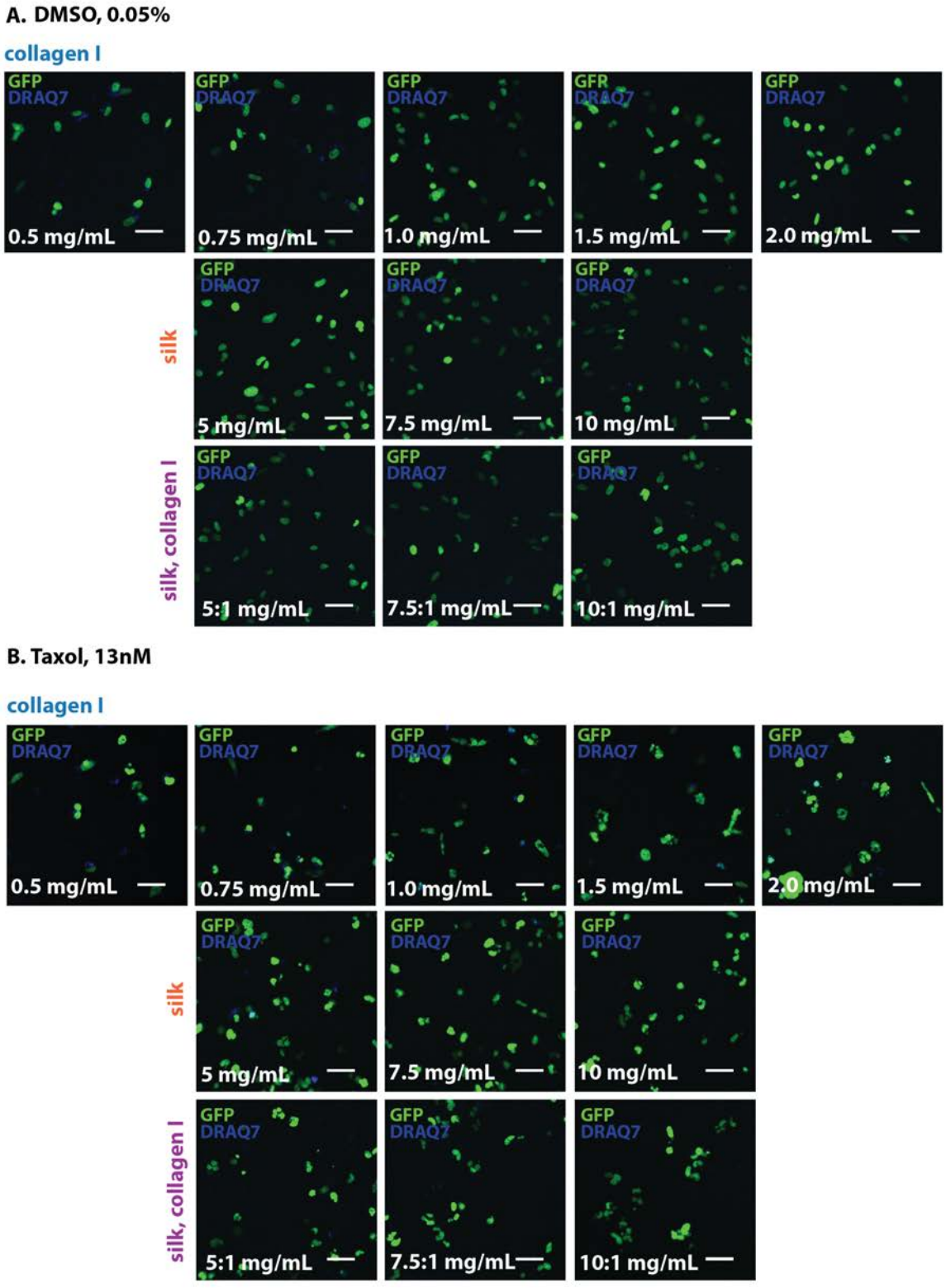

Figure S11: Immunofluorescent staining for all nuclei (green, GFP-H2B), and nuclei of dead cells with compromised membrane integrity (blue, DRAQ7). **A.** Viability in representative DMSO control wells. **B.** Viability in representative 13 nM Taxol treated wells.

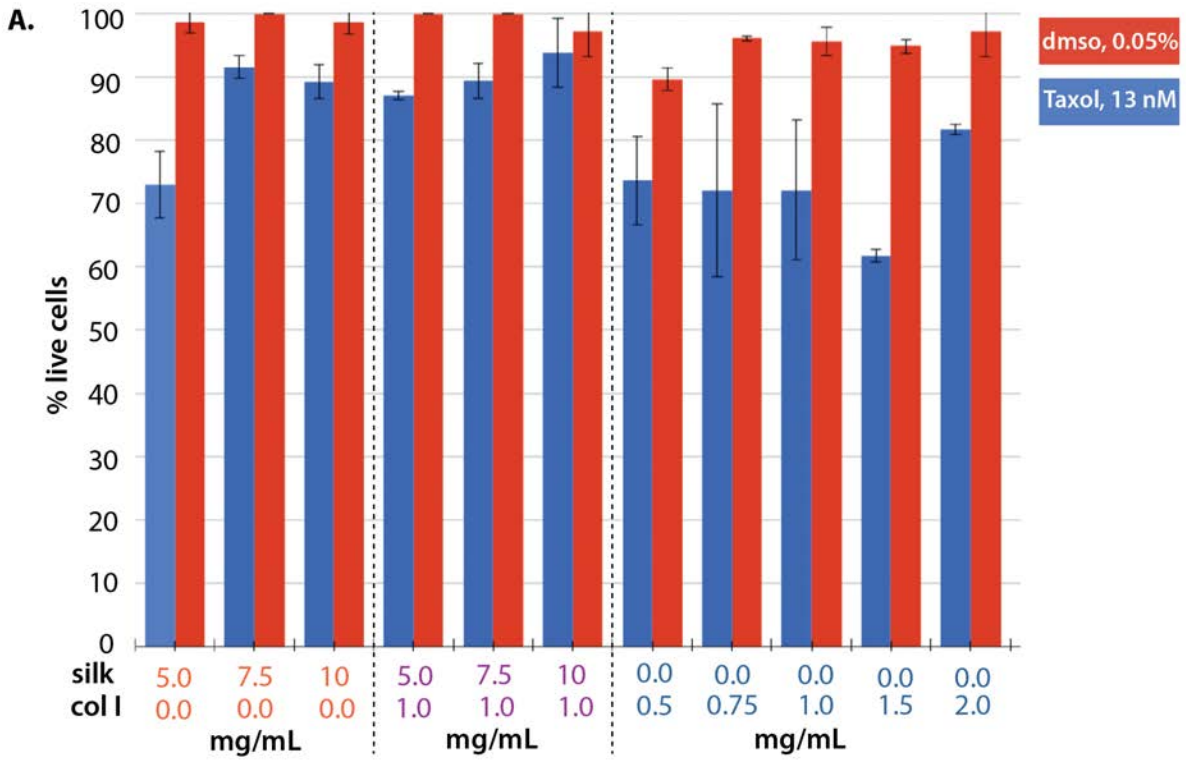

Figure S12: Cell viability quantified as percentage of live cells in representative area counted. Error bars: standard deviation

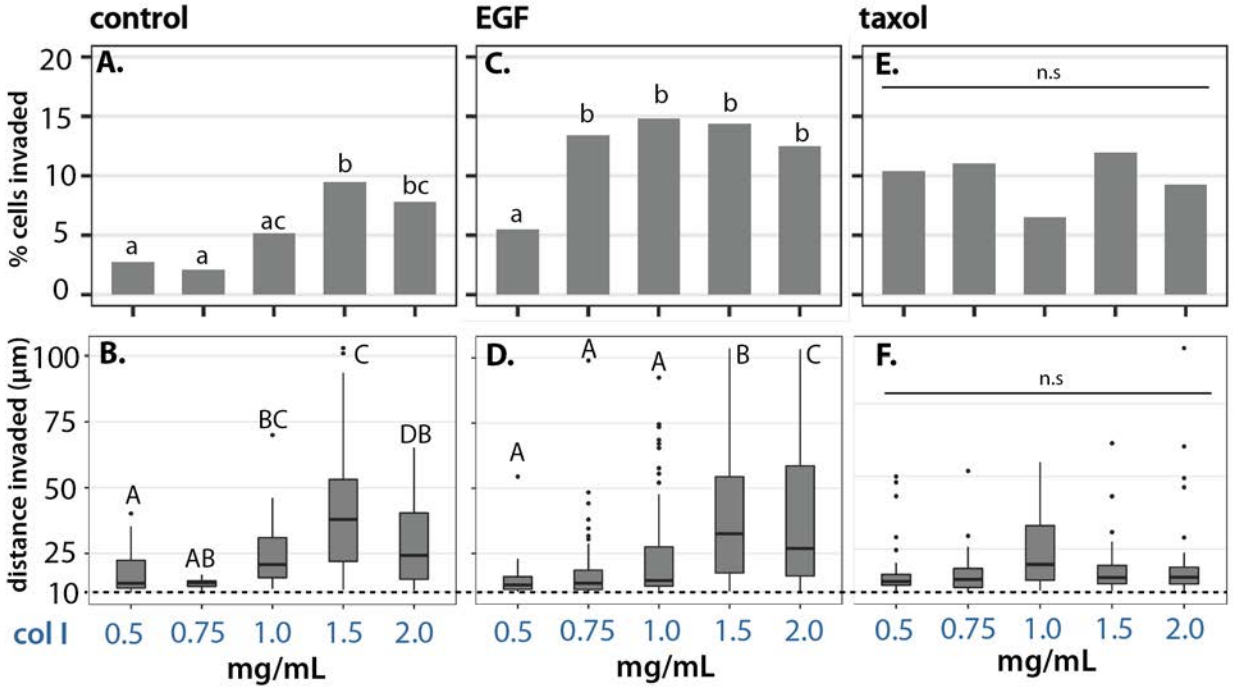

Figure S13: Percent of cells invaded (A.) in different collagen I concentrations only, in control media or 0.05% DMSO (Ai), with 8.33 nM EGF (A.), and 13 nM Taxol (C.). Box and violin plot of distances invaded in different collagen I concentrations only in control media or 0.05% DMSO (E.), with 8.33 nM EGF (D.), and 13 nM Taxol (F.). Boxplots show the median with lower (25%) and upper quartiles (75%). Whiskers further extend by 1.5X interquartile range from the lower and upper quartiles, with data points beyond this range plotted as outliers. Conditions with matching letter and style indicate non-significant differences with $p < 0.05$, based on Wilcoxon Krusal-Wallis test with non-parametric multiple comparisons.

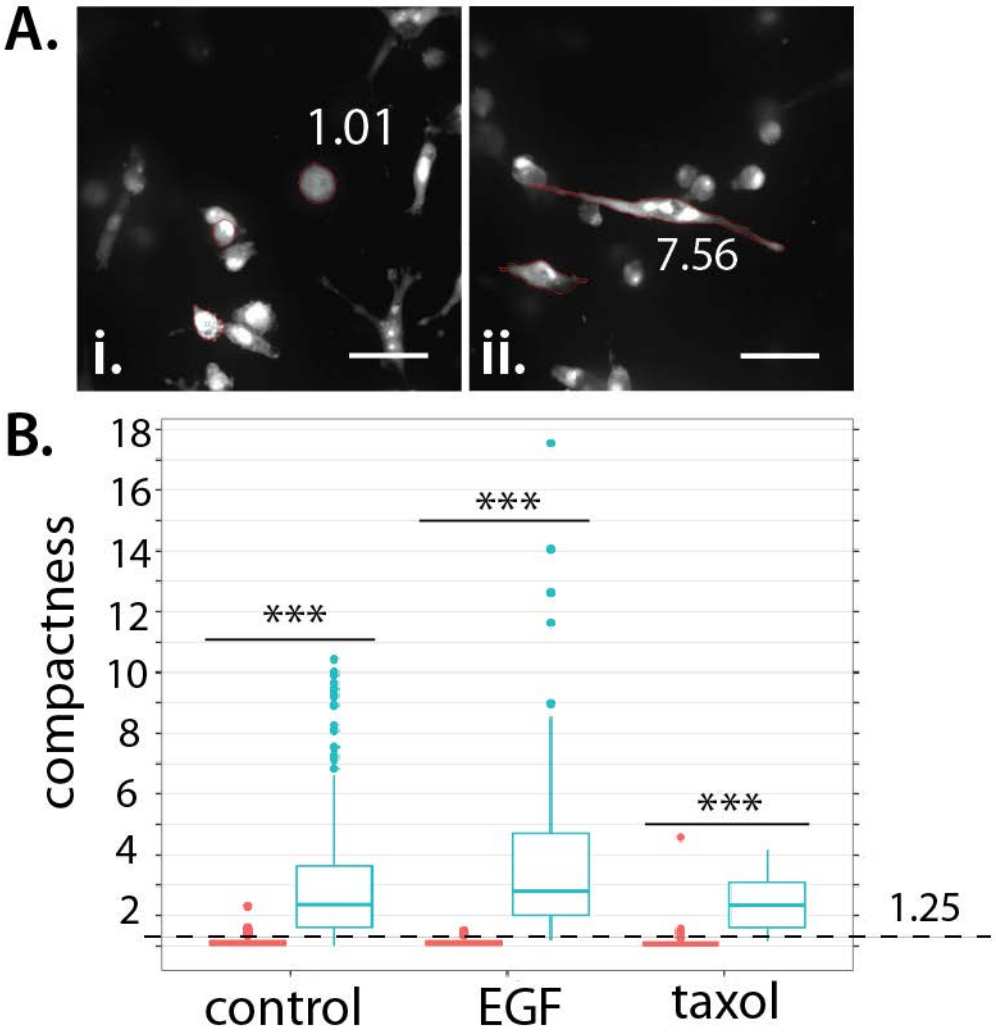

Figure S14: Representative amoeboid cell segmentation (Ai) and mesenchymal cell segmentation (Aii) and associated compactness value. Box plot of amoeboid vs. mesenchymal cells by compactness. Compactness metric significantly separates the segmented populations for all conditions. Cells classified as amoeboid in red, cells classified as mesenchymal in teal. Compactness value of 1.25 classifies mesenchymal and amoeboid populations with 89 and 88% accuracy, respectively.

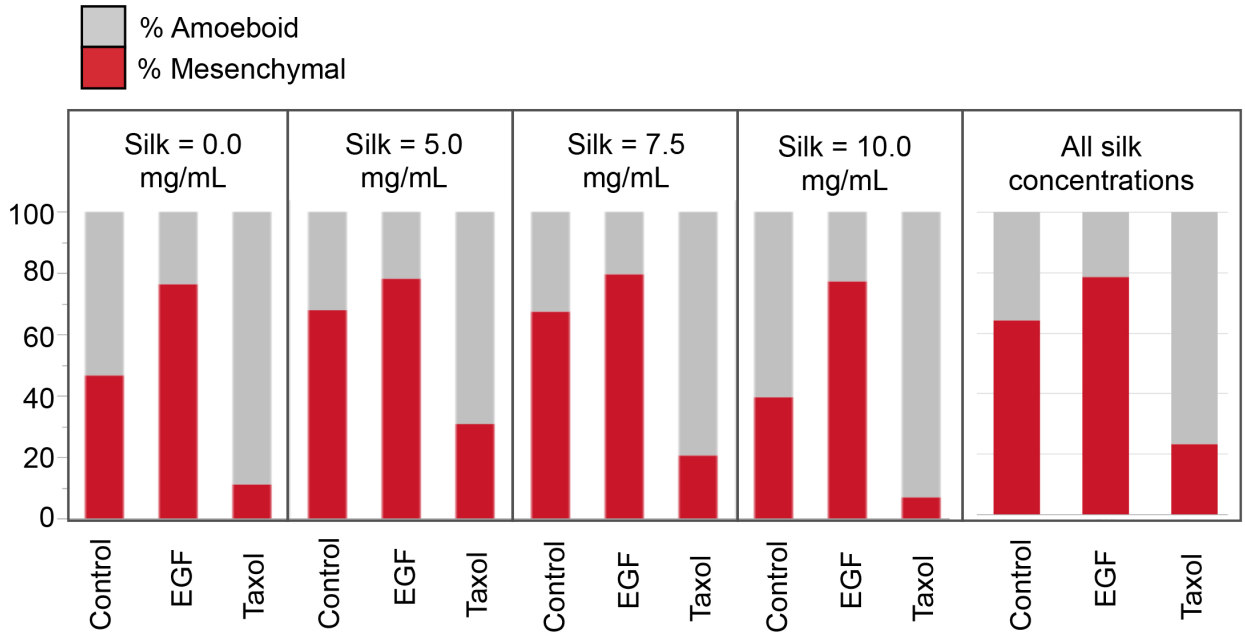

Figure S15: Representative mesenchymal (elongated) or amoeboid (compact) morphologies for cells in different silk fibroin concentrations only, and with 1 mg/mL collagen I in control media (A), with 8.33 nM EGF (B), and 13 nM Taxol (C). Percent cells with mesenchymal or amoeboid morphologies in collagen I only concentrations in control media (D), with 8.33 nM EGF (E), and 13 nM Taxol (F).

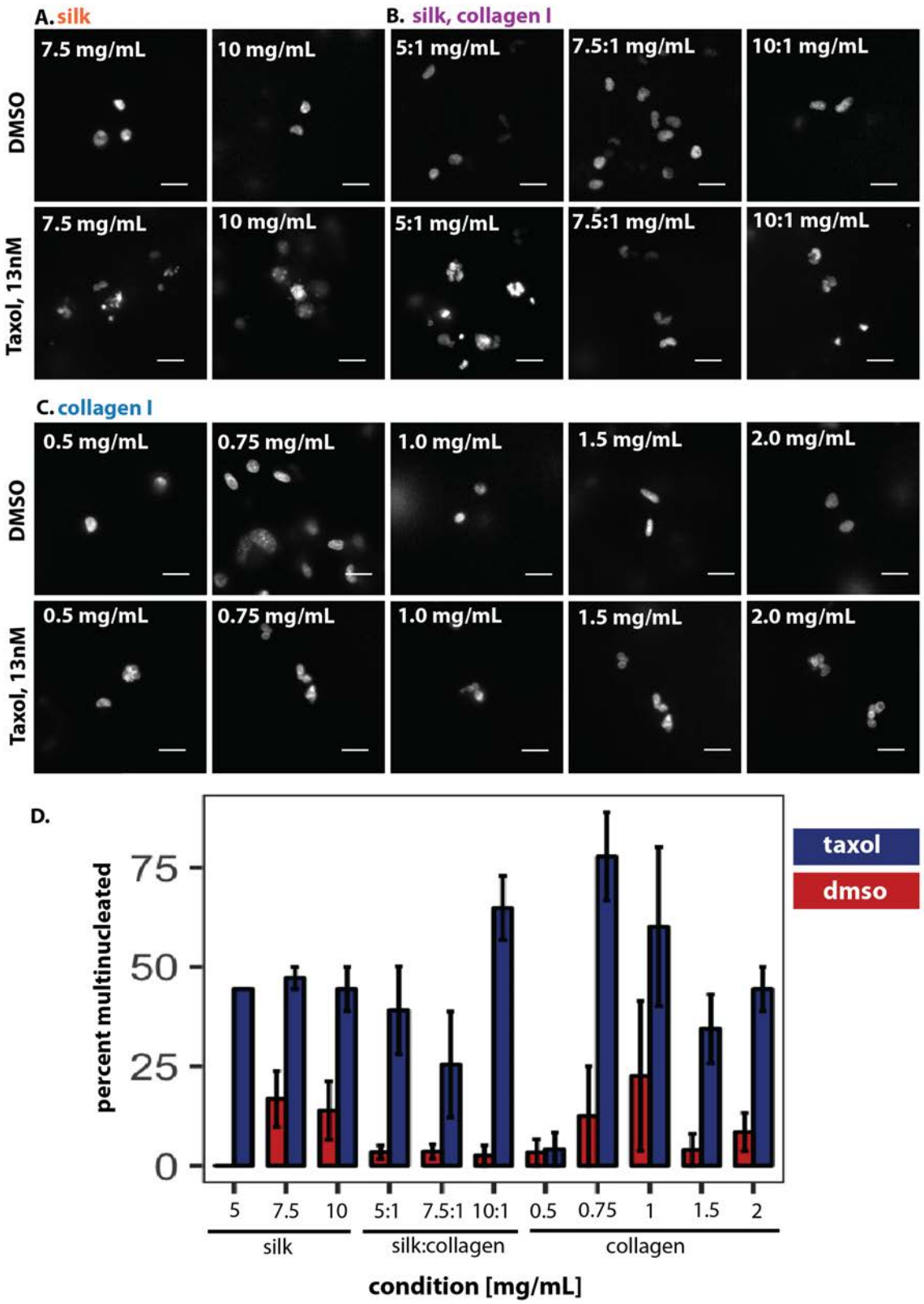

Figure S16: Representative images of nuclei morphologies in silk, silk collagen and collagen gels with and without taxol treatment. At 48 hours, taxol conditions have have significantly ($p < 0.0001$) more aberrant nuclei than their DMSO control for all conditions irrespective of hydrogel composition. Error bars: standard error of the mean.

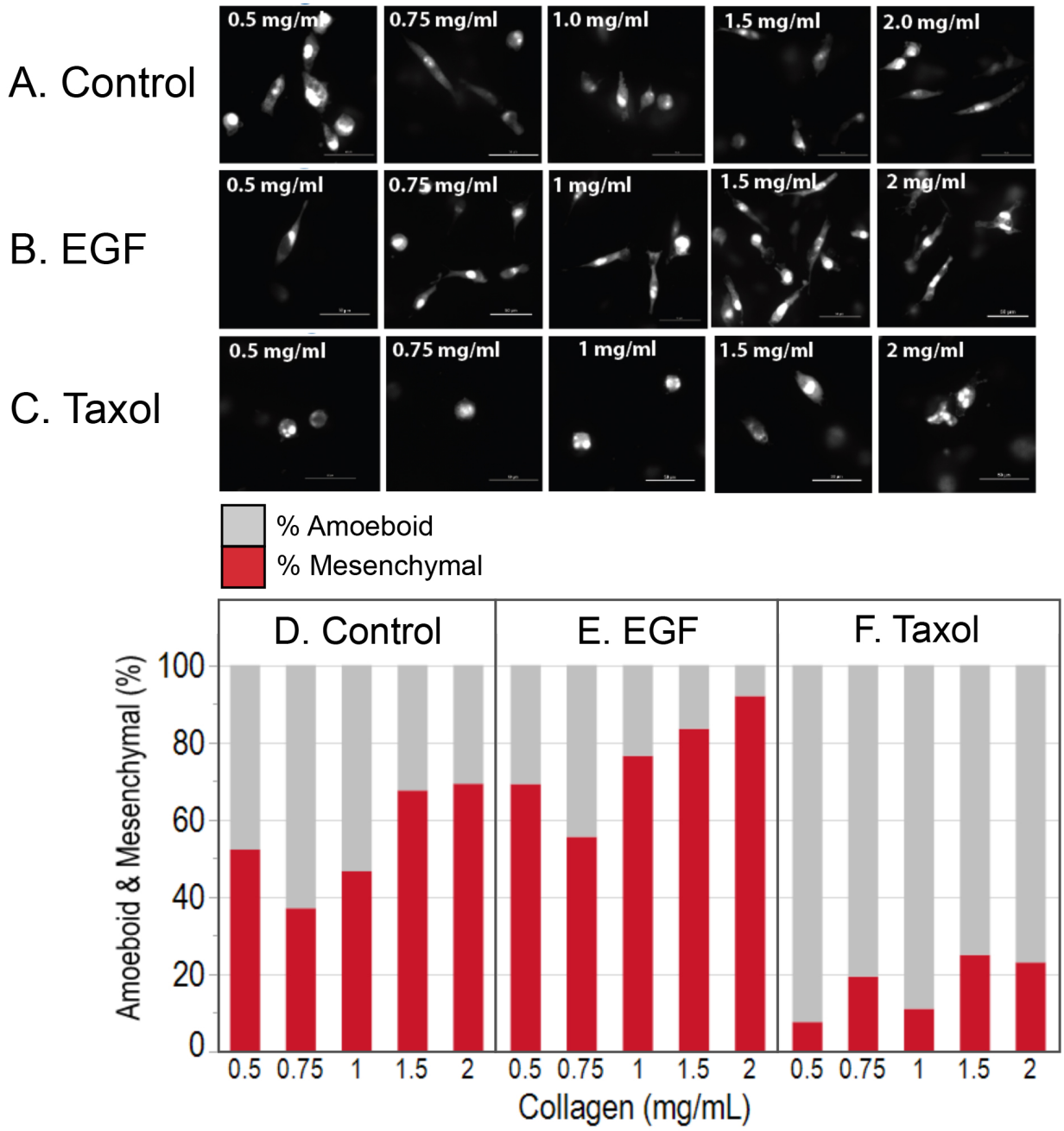

Figure S17: Representative mesenchymal (elongated) or amoeboid (compact) morphologies for cells in different collagen I concentrations only in control media (A), with 8.33 nM EGF (B), and 13 nM Taxol (C). Percent cells with mesenchymal or amoeboid morphologies in different collagen I concentrations in control media (D), with 8.33 nM EGF (E), and 13 nM Taxol (F).